J. Fluid Mech. (2010), *vol.* 651, *pp.* 241–250.
doi:10.1017/S0022112010000819

Cancellation exponents in helical and non-helical flows

P. RODRIGUEZ IMAZIO[1]† AND P. D. MININNI[1,2]

[1]Departamento de Física, Facultad de Ciencias Exactas y Naturales, Universidad de Buenos Aires and CONICET, Buenos Aires 1428, Argentina

[2]National Center for Atmospheric Research, P.O. Box 3000, Boulder, CO 80307, USA

(Received 11 August 2009; revised 30 December 2009; accepted 8 February 2010; first published online 9 April 2010)

Helicity is a quadratic invariant of the Euler equation in three dimensions. As the energy, when present helicity cascades to smaller scales where it dissipates. However, the role played by helicity in the energy cascade is still unclear. In non-helical flows, the velocity and the vorticity tend to align locally creating patches with opposite signs of helicity. Also in helical flows helicity changes sign rapidly in space. Not being a positive definite quantity, global studies considering its spectral scaling in the inertial range are inconclusive, except for cases where one sign of helicity is dominant. We use the cancellation exponent to characterize the scaling laws followed by helicity fluctuations in numerical simulations of helical and non-helical turbulent flows, with different forcing functions and spanning a range of Reynolds numbers from $\approx$670 to $\approx$6200. The exponent can be related to the fractal dimension as well as to the first-order helicity scaling exponent. The results are consistent with the geometry of helical structures being filamentary. Further analysis indicates that statistical properties of helicity fluctuations in the simulations do not depend on the global helicity of the flow.

1. Introduction

Theories of fully developed turbulence rely on the energy conservation in inviscid flows to derive the scaling laws of a turbulent system. However, energy is not the only quadratic invariant of the three-dimensional incompressible Euler equation, there is also the helicity

$$H = \int \mathrm{d}^3x\, \boldsymbol{v}(\boldsymbol{x}) \cdot \boldsymbol{w}(\boldsymbol{x}), \tag{1.1}$$

where $\boldsymbol{v}(\boldsymbol{x}, t)$ is the velocity field and $\boldsymbol{w}(\boldsymbol{x}, t) = \nabla \times \boldsymbol{v}$ is the vorticity field (Moffatt 1969). Helical motions are observed in a wide variety of geophysical flows, such as supercell convective storms which seem to owe their long life and stability to the helical nature of their circulation (Lilly 1986). In astrophysics it is well known that helicity plays a key role in the generation of large-scale magnetic fields through dynamo action (Pouquet, Frisch & Léorat 1976; Moffatt 1978). In hydrodynamic isotropic and homogeneous turbulence, recent studies of flows with net helicity confirmed that there is a joint cascade of energy an helicity to smaller scales (Borue & Orszag 1997; Chen, Chen & Eyink 2003*a*; Gomez & Mininni 2004), as expected from theoretical arguments (Brissaud *et al.* 1973). In the case of non-helical flows, velocity

† Email address for correspondence: paolaimazio@df.uba.ar

and vorticity tend to align locally creating patches of strong positive and negative helicities. In helical flows, helicity still fluctuates strongly around its mean value, both in space and time, creating localized patches with helicity much larger or smaller than the mean. As helicity is not positive definite, the study of its turbulent fluctuations is difficult and has received less attention. The scaling laws followed by helical fluctuations are unclear, and few comparisons are available between helical and non-helical flows to understand their impact on the energy cascade. The development of helical structures on turbulent flows has been discussed by Moffatt (1985) and it has also been proposed that such structures may have an impact on the dynamics of turbulent flows as helical regions have the velocity and vorticity aligned, with a resulting quenching of the nonlinear term in the Navier–Stokes equations (Moffatt & Tsinober 1992). Intermittency in the helicity flux has also been recently studied in numerical simulations (Chen *et al.* 2003*b*), and the geometry of helical structures was considered using wavelet decompositions (Farge, Pellegrino & Schneider 2001) and Minkowski functionals in the magnetohydrodynamics case (Wilkin, Barenghi & Shukurov 2007).

In this work we use the cancellation exponent (Ott *et al.* 1992) to study the fast fluctuations of helicity in turbulent helical and non-helical flows. The cancellation exponent was introduced to study fast changes in sign of fields on arbitrarily small scales, and is based on the study of the inertial range scaling of a generalized partition function built on a signed measure. Under some conditions, it was shown to be related to the fractal dimension of structures in the flow and to the Holdër exponent (Vainshtein *et al.* 1994). It was used to characterize fluctuations in hydrodynamic turbulence and magnetohydrodynamic dynamos (Ott *et al.* 1992), as well as in two-dimensional magnetohydrodynamic turbulence (Sorriso-Valvo *et al.* 2002; Pietarila Graham, Mininni & Pouquet 2005). In solar wind observations it was used to show that magnetic helicity is sign singular (Bruno & Carbone 1997). However, to the best of our knowledge, no studies of helical fluctuations in hydrodynamic turbulence have been done using the cancellation exponent. The main motivation of our work is then to use the cancellation exponent as a diagnostic tool, to compare its behaviour in the helical and non-helical flows. In this sense, our results should be interpreted in the light of similar studies in magnetohydrodynamic turbulence. Little is known of pointwise properties of the solutions of the Stokes equations (see e.g. Eyink & Sreenivasan 2006), and beyond characterization of helicity fluctuations, other results should be considered in a phenomenological fashion. We analyse data stemming from direct numerical simulations (DNSs) of the Navier–Stokes equations in a three-dimensional periodic box at large resolutions (up to 1024^3 grid points) with different external mechanical forcing. Both helical and non-helical flows are considered. Results stemming from the cancellation exponent analysis indicate that the scaling properties of helicity fluctuations in the simulations are independent of the net helicity of the flow. The results also suggest that helicity fluctuations may be sign singular. Bearing in mind the previously discussed limitations we obtain a relation from phenomenological arguments between the helicity cancellation exponent, the fractal dimension of helical structures and the first-order scaling exponent of helicity.

2. The cancellation exponent

The cancellation exponent (Ott *et al.* 1992) was introduced to characterize the behaviour of measures that take both positive and negative values, and to quantify a form of singularity where changes in sign occur on arbitrarily small scales. We can

introduce the cancellation exponent for the helicity considering a hierarchy $Q_i(l)$ of disjoint subsets of size l covering the entire domain occupied by the fluid $Q(L)$ of size L. For each scale l, a signed measure of helicity is introduced as

$$\mu_i(l) = \int_{Q_i(l)} \mathrm{d}^3x\ H(\boldsymbol{x}) \Big/ \int_{Q(L)} \mathrm{d}^3x\ |H(\boldsymbol{x})|, \tag{2.1}$$

where $H(\boldsymbol{x}) = \boldsymbol{v}(\boldsymbol{x}) \cdot \boldsymbol{w}(\boldsymbol{x})$ is the helicity density such that the total helicity is $H = \int \mathrm{d}^3x H(\boldsymbol{x})$. Since the normalization factor in (2.1) is the integral of the absolute value of H over the entire domain, the signed measure is bounded between 1 and -1 and can be interpreted as the difference between two probability measures, one for the positive component and another for the negative component of the helicity density. To study cancellations at a given length scale, we build the partition function

$$\chi(l) = \sum_{Q_i(l)} |\mu_i(l)|. \tag{2.2}$$

In the inertial range, the scaling law followed by the cancellations can be studied by fitting

$$\chi(l) \sim l^{-\kappa}, \tag{2.3}$$

where κ is the cancellation exponent. This exponent represents a quantitative measure of the cancellation efficiency. If such a scaling law exists and its range increases as the inertial range increases, the signed measure is called sign singular. In this case, changes in sign occur everywhere and in any scale considered in the limit of infinite Reynolds number. On the other hand, for a completely smooth field no fast oscillations in sign will occur below a certain scale, leading to $\chi(l) = 1$ and therefore $\kappa = 0$.

3. Code and numerical simulations

The data we use for the analysis stems from DNS of the incompressible Navier–Stokes equations with constant mass density,

$$\frac{\partial \boldsymbol{v}}{\partial t} + \boldsymbol{v} \cdot \nabla \boldsymbol{v} = -\nabla p + \nu \nabla^2 \boldsymbol{v} + \boldsymbol{f}, \tag{3.1}$$

$$\nabla \cdot \boldsymbol{v} = 0, \tag{3.2}$$

where $\boldsymbol{v}$ is the velocity field, p is the pressure (divided by the mass density), ν is the kinematic viscosity and $\boldsymbol{f}$ represents an external force that drives the turbulence (Pope 2000).

For the analysis, we consider six numerical simulations at different Reynolds numbers and spatial resolutions, with different forcing functions that inject either energy or both energy and helicity. The simulations are listed in table 1 and described in more detail in a previous paper (Mininni, Alexakis & Pouquet 2006). Spatial resolutions range from 256^3 to 1024^3 grid points, with Reynolds numbers $R_e = UL/\nu$ (with U the root mean square (r.m.s.) velocity and L the integral scale) ranging from $\approx$675 to $\approx$6200, and Taylor–Reynolds numbers $R_e = U\lambda/\nu$ (where λ is the Taylor scale) ranging from $\approx$300) to $\approx$1100. Two forcing functions were considered: Taylor–Green (TG) forcing, which injects no helicity in the flow (although helicity fluctuations around zero develop as a result of nonlinearities in the Navier–Stokes equations), and Arn'old–Beltrami–Childress (ABC) forcing, which injects maximum (positive) helicity in the flow. The forcings were applied respectively in the shells in Fourier space with wavenumber $k_F = 2$ and 3. All runs were continued for over ten turnover times after

Run	N	$\boldsymbol{F}$	k_F	ρ_H	ν	R_e	R_λ
T1	256	TG	2	0.03	2×10^{-3}	675	300
T2	512	TG	2	0.01	1.5×10^{-3}	875	350
T3	1024	TG	2	0.03	3×10^{-4}	3950	800
A1	256	ABC	3	0.79	2×10^{-3}	820	360
A2	512	ABC	3	0.81	2.5×10^{-4}	2520	670
A3	1024	ABC	3	0.83	2.5×10^{-4}	6200	1100

TABLE 1. Runs used for the analysis. N is the linear grid resolution, $\boldsymbol{F}$ is the forcing, either Taylor–Green (TG) or Arn'old–Beltrami–Childress (ABC), k_F is the forcing wavenumber, ρ_H is the relative helicity, ν is the kinematic viscosity, R_e is the Reynolds number and R_λ is the Reynolds number based on the Taylor scale.

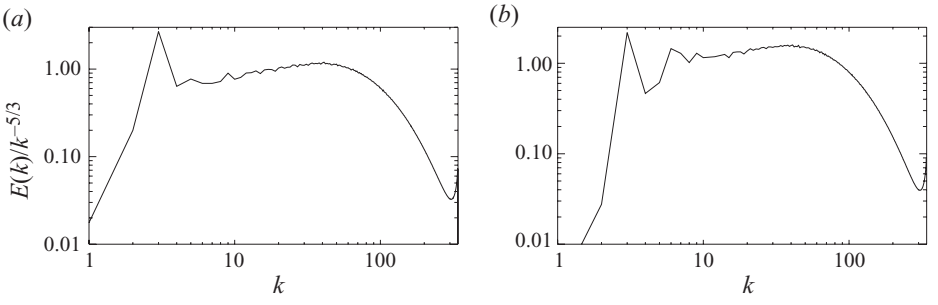

FIGURE 1. Energy spectrum compensated with the Kolmogorov $k^{-5/3}$ scaling law, for the A3 (a) and T3 (b) runs.

reaching the turbulent steady state. As a measure of the helicity content of each flow, we computed a relative helicity $\rho_H = H/(k_F E)$ (where E is the total energy) averaged in time over the turbulent steady state of each run (see table 1).

4. Results and analysis

To study scaling laws of helicity fluctuations in the inertial range of helical and non-helical flows, we performed a signed measure analysis and computed the cancellation exponent κ for all runs. Following (2.3), this can be done by computing $\chi(l)$ and fitting $\chi(l) \sim l^{-\kappa}$ in the inertial range.

Although a detailed analysis of the simulations can be found in Mininni *et al.* (2006), in figure 1 we show as a reference the compensated energy spectrum of the two simulations at the largest Reynolds numbers attained (runs A3 and T3). The spectra present a short inertial range followed by a bottleneck, as is usual in simulations of hydrodynamic turbulence. The runs also have a range with approximately constant energy flux, as well as a range of scales consistent with Kolmogorov 4/5 law (Kolmogorov 1941; Frisch 1995) when third-order structure functions are computed. As usual, these ranges have slightly different extensions depending on the quantity studied, and it will be shown that the cancellation exponent shows a scaling range comprised between $l \approx 0.08$ and 0.7, which correspond roughly to wavenumbers between $k \approx 8$ and 80, which is wider than but includes the inertial range of both runs. At the lower resolution, the inertial range in the energy spectrum and flux, or in the third-order structure function, is shorter and harder to identify.

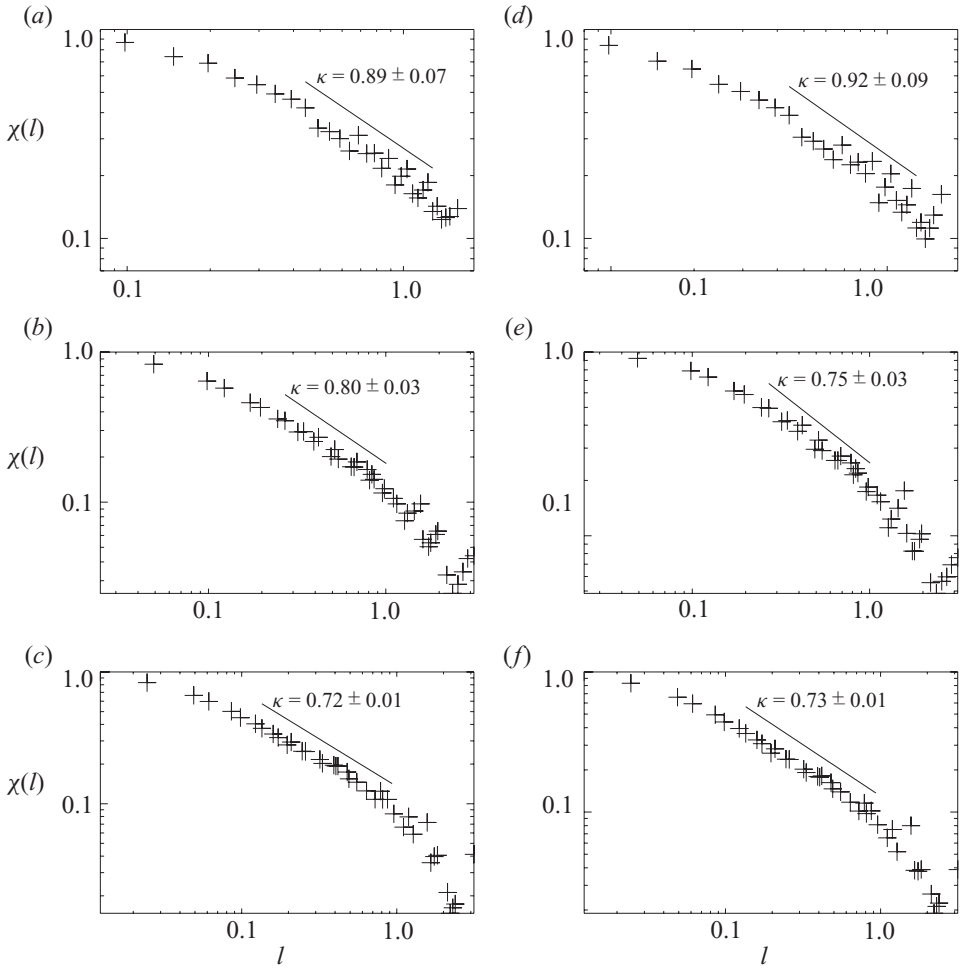

FIGURE 2. Signed measure of helicity as a function of the scale for runs with increasing resolution: TG forcing (*a–c*) and ABC forcing (*d–f*) after subtracting the mean value of helicity. Slopes with the cancellation exponent are given as a reference.

Figure 2(*a–c*) shows the signed measure of helicity as a function of the scale for runs T1, T2 and T3 from top to bottom (non-helical, with increasing Reynolds numbers). As the Reynolds number increases, a wider scaling range can be identified. The values obtained for the cancellation exponent are $\kappa = 0.92 \pm 0.09$, 0.75 ± 0.03 and 0.73 ± 0.01 respectively for runs T1, T2 and T3. The values obtained and the dependence with Reynolds number hints that in the limit of vanishing viscosity, helicity fluctuations may be sign singular, i.e. that fast changes in sign of helicity may occur everywhere in arbitrarily small scales in the flow. This result is consistent with helicity cascading towards small scales, and with observations of the helicity distribution being highly intermittent (Chen *et al.* 2003*b*) (albeit the previous studies are only for flows with net helicity).

As mentioned earlier, the flows with ABC forcing are helical. For such flows the direct cascade of helicity and its intermittency has been studied before using spectral quantities. Although helicity fluctuations develop in these flows, given the predominant sign of helicity, fluctuations occur around the mean value and less changes in sign

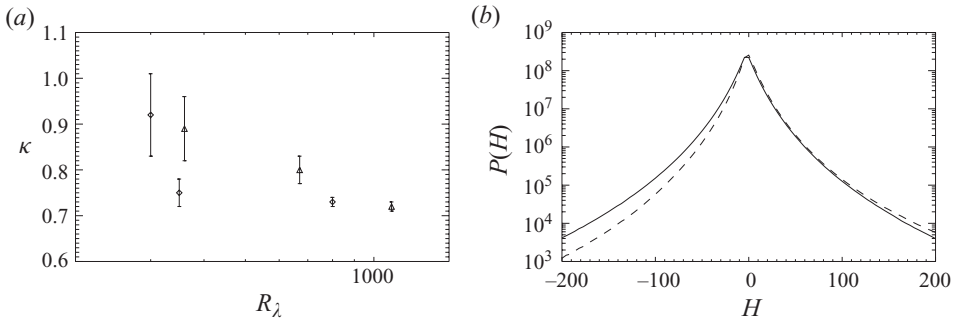

FIGURE 3. (*a*) Cancellation exponent κ as a function of the Taylor-based Reynolds numbers for the helical (triangles) and the non-helical (diamonds) flow. (*b*) Histogram of helicity fluctuations for the T3 (solid) and A3 (dashed) runs.

take place. Indeed, if the signed measure of helicity and the cancellation exponent is computed for run A3, we obtain $\kappa = 0.26 \pm 0.04$. This smaller value of the exponent is consistent with the less number of cancellations, and the larger error is associated to the fact that larger fluctuations are observed in the signed measure as less events with changes of sign are available. However, we are interested in helicity fluctuations around the mean value, and to correctly consider these fluctuations the mean value of helicity H was subtracted from the helicity density in runs A1, A2 and A3 prior to the analysis. The resulting signed measures are also shown in figure 2(*d–f*). In this case we also observe scaling of $\chi(l)$ expanding over a wider range of scales as the Reynolds number increases.

The results obtained for the helicity cancellations in helical and non-helical runs are similar. The cancellation exponents are $\kappa = 0.89 \pm 0.07$, 0.80 ± 0.03 and 0.72 ± 0.01 respectively for runs A1, A2 and A3. At the highest resolution three ranges can be identified in both the A3 and T3 runs. At the smaller scales, viscous effects dominate and the flow is smooth. This results in less changes of sign in helicity and a shallower distribution of the signed measure. The slope tends to zero, as expected for a smooth flow, and the signed measure tends to one for the smallest resolved scale. At intermediate scales an inertial range is observed, and at larger scales the results are affected by the external forcing. In these scales, large fluctuations in the value of $\chi(l)$ are observed as a result. As mentioned before, the inertial range of $\chi(l)$ is wider than the inertial range observed in the energy spectrum. This is consistent with observations of the helicity spectrum decaying slower than the energy spectrum near the dissipative range in helical turbulence (Mininni *et al.* 2006).

The cancellation exponent obtained in all runs as a function of the Taylor based Reynolds number is shown in figure 3(*a*). For both the helical and non-helical runs κ decreases with the Reynolds number, and for the largest Reynolds numbers studied the value of κ seems to saturate and is the same within error bars for both helical and non-helical flows. Note that because of the different forcing functions, the helical and non-helical runs have slightly different Reynolds numbers even when the same grid resolution is used. The similarities between the scaling laws of the helical and non-helical flows suggest that statistics of the helicity fluctuations are the same in both cases. This is further confirmed by a histogram of the helicity fluctuations around its mean value for the T3 and A3 runs. As figure 3(*b*) shows, turbulent fluctuations of helicity are similar, with small differences in the tails.

The power laws observed suggest that helicity fluctuations may be sign singular. The fast oscillations in sign point to a highly intermittent quantity that fluctuates rapidly in localized structures at arbitrarily small scales for very large Reynolds numbers. As mentioned in the introduction, the cancellation exponent can be related to the geometry of such structures, and under some conditions these relations can be rigorously derived (Vainshtein *et al.* 1994). However, considering how little is known about the solutions of the Navier–Stokes equations, we choose instead to derive the relations using simple geometrical and phenomenological arguments. In the following, we extend the analysis of Sorriso-Valvo *et al.* (2002) for the current density in magnetohydrodynamics to consider the case of kinetic helicity in hydrodynamic turbulence. We assume the helicity is spatially correlated (although not necessarily locally smooth) in D dimensions and uncorrelated in $3-D$ dimensions, where 3 follows from the dimension of the space. With this choice, a correlated helicity distribution has $D=3$, and a completely uncorrelated helicity distribution has $D=0$. For intermediate cases, we can estimate the signed measure of helicity as follows:

$$\chi(l)=\sum_{Q_i(l)}\left|\int_{Q_i(l)}\mathrm{d}^3x\,H(\boldsymbol{x})\Big/\int_{Q(L)}\mathrm{d}^3x\,|H(\boldsymbol{x})|\right|\sim\frac{1}{L^3\langle H^2\rangle^{1/2}}\left(\frac{L}{l}\right)^3\left|\int_{Q(l)}\mathrm{d}^3x\,H(\boldsymbol{x})\right|, \quad (4.1)$$

where we used homogeneity to replace the sum over all subsets $Q_i(l)$ by $(L/l)^3$ (the total number of terms in the sum) times the integral over a generic box $Q(l)$ of size l. Since the absolute values in the denominator prevent any cancellation, the integral below was approximated by the characteristic value L^3H_{rms} where $H_{rms}=\langle H^2\rangle^{1/2}$ is the r.m.s. value of the helicity density.

In the inertial range, and still under homogeneity assumptions, the helicity follows some scaling law which can be represented by helicity structure functions $\langle\delta H(s)\rangle\sim s^h$, where $s=|\boldsymbol{s}|$ represents a lineal increment. We can then split the integral over the domain $Q(l)$ in integrals over subdomains with volume λ^3 such that they separate the contributions from domains where the helicity is correlated of domains where the helicity is uncorrelated in space. Then, the remaining integral in (4.1) can be estimated as (Sorriso-Valvo *et al.* 2002)

$$\left|\int_{Q(l)}\mathrm{d}^3x\;H(\boldsymbol{x})\right|\sim\langle H^2\rangle^{1/2}\int_{Q(l)}\mathrm{d}^Ds\left(\frac{s}{\lambda}\right)^h\int_{Q(l)}\mathrm{d}^{3-D}s. \quad (4.2)$$

The uncorrelated dimensions give a value proportional to the square root of their volume $(l/\lambda)^{(3-D)/2}$. The correlated dimensions give a contribution proportional to $(l/\lambda)^{h+D}$, which for $h=0$ (locally smooth helicity) is proportional to their volume. Replacing these expressions in (4.1), we get that the signed measure of helicity $\chi(l)$ scales as

$$\chi(l)\sim l^{-\left(\frac{3-D}{2}-h\right)}. \quad (4.3)$$

Thus the cancellation exponent κ, the fractal dimension D and the scaling exponent h are related through

$$\kappa=\frac{3-D}{2}-h. \quad (4.4)$$

A completely smooth field ($D=3$) has $\kappa=h=0$, in agreement with the definition of κ and of the first-order (Hölder) scaling exponent h for the field (see Bruno & Carbone 1997; Sorriso-Valvo *et al.* 2002). In a turbulent flow, the global helicity is observed to follow Kolmogorov scaling, and therefore we can assume $h=1/3$ (Kurien 2003; Mininni *et al.* 2006). Then from the value of $\kappa=0.73\pm0.01$ it follows that

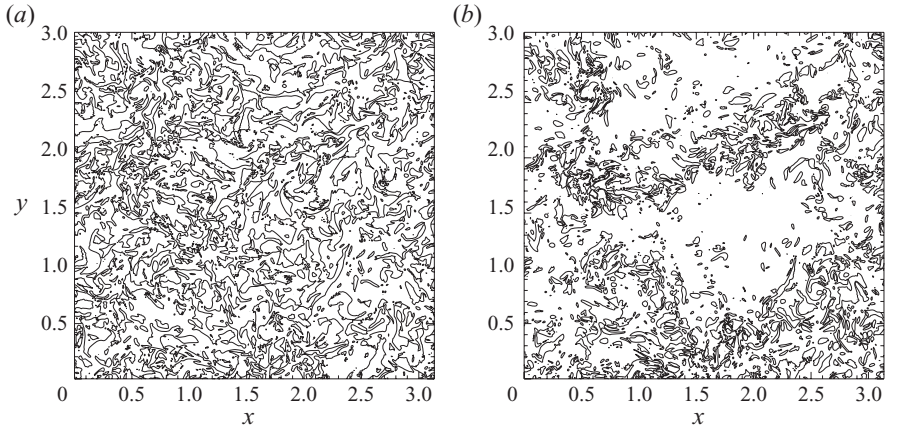

FIGURE 4. Contour levels of helicity density in a slice of the T3 run. Only 1/4 of the slice is shown. (*a*) Contours with $H(\boldsymbol{x}) = 0$, i.e. places where cancellations take place. (*b*) Contours with $H(\boldsymbol{x}) = 12$. Note how contour levels of zero helicity fill the space, while white patches are observed in the contour levels of non-zero helicity, as well as filamentary structures.

helical structures are filamentary with fractal dimension $D = 0.873 \pm 0.005$, in good agreement with previous observations of helical vortex filaments (Moffatt & Tsinober 1992; Farge *et al.* 2001; Chen *et al.* 2003*b*; Mininni *et al.* 2006; Holm & Kerr 2007; Baerenzung *et al.* 2008). As an illustration, figure 4 shows a slice of the helicity density in the T3 run. Filamentary structures can be identified, specially for the contour levels corresponding to large concentration of helicity. Structures less elongated were confirmed to correspond to filaments that cross the slice perpendicularly.

5. Conclusions

Signed measures of helicity were calculated for turbulent flows with different Reynolds numbers and helicity contents. For both helical and non-helical flows cancellation exponents were calculated, obtaining a value compatible with $\kappa = 0.73 \pm 0.01$ for helicity fluctuations for both cases at the largest Reynolds number considered. This is the main result of our work, indicating that the cancellation exponent may be a useful tool to characterize scaling laws followed by helicity fluctuations in hydrodynamic turbulence.

The scaling range of $\chi(l)$ increases with the Reynolds number, and the value of the cancellation exponent obtained suggest that helicity may be sign singular in the limit of infinite Reynolds number. However, note that a possible decrease of the cancellation exponent as $\sim 1/\log(R_\lambda)$ cannot be ruled out from the numerical data, specially for the runs with ABC forcing.

Simple geometrical arguments were used to link the cancellation exponent κ to the fractal dimension D of the structures. To do this we assumed a single-scaling exponent h for the lineal helical increments. Assuming $h = 1/3$, a value consistent with numerical results, we obtain that helicity fluctuations are filamentary with fractal dimension of $D = 0.873 \pm 0.005$, also in agreement with observations. Such a picture of a turbulent flow with filamentary helical structures of opposite sign separating regions with zero helicity is consistent with arguments put forwards by Moffatt (1985). However, these final results, based on the analysis of numerical data and on

phenomenological arguments, should only be considered as intriguing and provocative until more is known about formal properties of the solutions of the Navier–Stokes equations.

The authors acknowledge support from Grants No. UBACYT X468/08 and PICT-2007-02211. P. D. Mininni acknowledges support from the Carrera del Investigador Científico of CONICET.

REFERENCES

Baerenzung, J., Politano, H., Ponty, Y. & Pouquet, A. 2008 Spectral modelling of turbulent flows and the role of helicity. *Phys. Rev.* E **77**, 046303.

Borue, V. & Orszag, S. A. 1997 Spectra in helical three-dimensional homogeneous isotropic turbulence. *Phys. Rev.* E **55**, 7005–7009.

Brissaud, A., Frisch, U., Léorat, J., Lesieur, M. & Mazure, A. 1973 Helicity cascades in fully developed isotropic turbulence. *Phys. Fluids* **16**, 1366–1367.

Bruno, R. & Carbone, V. 1997 Sign singularity of the magnetic helicity from in situ solar wind observations. *Astrophys. J.* **488**, 482–487.

Chen, Q., Chen, S. & Eyink, G. 2003*a* The joint cascade of energy and helicity in three-dimensional turbulence. *Phys. Fluids.* **15**, 361–374.

Chen, Q., Chen, S., Eyink, G. & Holm, D. 2003*b* Intermittency and the joint cascade of energy and helicity. *Phys. Rev. Lett.* **90**, 214503.

Eyink, G. & Sreenivasan, K. 2006 Onsager and the theory of hydrodinamic turbulence. *Rev. Mod. Phys.* **78**, 87–134.

Farge, M., Pellegrino, G. & Schneider, K. 2001 Coherent vortex extraction in 3D turbulent flows using orthogonal wavelets. *Phys. Rev. Lett.* **87**, 054501.

Frisch, U. 1995 *Turbulence*. Cambridge University Press.

Gomez, D. O. & Mininni, P. D. 2004 Understanding turbulence through numerical simulations. *Physica* A **342**, 69–75.

Holm, D. & Kerr, R. 2007 Helicity in the formation of turbulence. *Phys. Fluids* **19**, 025101.

Kolmogorov, A. N. 1941 The local structure of turbulence in incompressible viscous fluid for very large Reynolds number. *Dokl. Acad. Nauk SSSR* A **30**, 301–305.

Kurien, S. 2003 The reflection-antisymmetric counterpart of the Kármán–Howarth dynamical equation. *Physica* D **175**, 167–176.

Lilly, D. 1986 The structure, energetics and propagation of rotating convective storms. *J. Atmos. Sci.* **43**, 126–140.

Mininni, P., Alexakis, A. & Pouquet, A. 2006 Large scale flow effects, energy transfer, and self-similarity on turbulence. *Phys. Rev.* E **74**, 016303.

Moffatt, H. K. 1969 The degree of knottedness of tangled vortex lines. *J. Fluid Mech.* **35**, 117–129.

Moffat, H. K. 1978 *Magnetic Field Generation in Electrically Conducting Fluids.* Cambridge University Press.

Moffatt, H. K. 1985 Magnetostatic equilibria and analogous Euler flows of arbitrarily complex topology. *J. Fluid Mech.* **159**, 359–378.

Moffatt, H. K. & Tsinober, A. 1992 Helicity in laminar and turbulent flows. *Annu. Rev. Fluid Mech.* **24**, 281–312.

Ott, E., Du, Y., Sreenivasan, K., Juneja, A. & Suri, A. 1992 Sign-singular measures: fast magnetic dynamos, and high-Reynolds-number fluid turbulence. *Phys. Rev. Lett.* **69**, 2654–2657.

Pietarila Graham, J., Mininni, P. D. & Pouquet, A. 2005 Cancellation exponent and multifractal structure in two-dimensional magnetohydrodynamics: direct numerical simulations and Lagrangian averaged modelling. *Phys. Rev.* E **72**, 045301(R).

Pope, S. 2000 *Turbulent Flows.* Cambridge University Press.

Pouquet, A., Frisch, U. & Léorat, J. 1976 Strong MHD helical turbulence and the nonlinear dynamo effect. *J. Fluid Mech.* **77**, 321–354.

Sorriso-Valvo, L., Carbone, B., Noullez, A., Politano, H., Pouquet, A. & Veltri, P. 2002 Analisys of cancellation in two-dimensional magnetohydrodinamic turbulence. *Phys. Plasmas* **9**, 89–95.

Vainshtein, S. I., Sreenivasan, K. R., Pierrehumbert, R. T., Kashyap, V. & Juneja, A. 1994 Scaling exponents for turbulence and other random processes and their relationships with multifractal structure. *Phys. Rev.* E **50**, 1823–1835.

Wilkin, L. S., Barenghi, C. F. & Shukurov, A. 2007 Magnetic structures produced by small-scale dynamos. *Phys. Rev. Lett.* **99**, 134501.